

Stress States in Highly Flexible Thin-Walled Composite Structures by Unified Shell Model

*Original*

Stress States in Highly Flexible Thin-Walled Composite Structures by Unified Shell Model / Pagani, Alfonso; Azzara, Rodolfo; Augello, Riccardo; Carrera, Erasmo. - In: AIAA JOURNAL. - ISSN 0001-1452. - STAMPA. - 59:10(2021), pp. 4243-4256. [10.2514/1.J060024]

*Availability:*

This version is available at: 11583/2928732 since: 2021-10-02T16:26:31Z

*Publisher:*

AIAA

*Published*

DOI:10.2514/1.J060024

*Terms of use:*

openAccess

This article is made available under terms and conditions as specified in the corresponding bibliographic description in the repository

*Publisher copyright*

(Article begins on next page)

# Stress states in highly flexible thin-walled composite structures by unified shell model

Alfonso Pagani<sup>\*</sup>, Rodolfo Azzara<sup>†</sup>, Riccardo Augello<sup>‡</sup>  
*MUL<sup>2</sup> group, Department of Mechanical and Aerospace Engineering,  
Politecnico di Torino, Corso Duca degli Abruzzi 24, 10129 Torino, Italy.*

Erasmus Carrera<sup>§</sup>  
*MUL<sup>2</sup> group, Department of Mechanical and Aerospace Engineering,  
Politecnico di Torino, Corso Duca degli Abruzzi 24, 10129 Torino, Italy.*  
*Department of mechanical engineering, college of engineering,  
Prince Mohammad Bin Fahd University P.O. Box 1664. Al Khobar 31952. Kingdom of Saudi Arabia.*

**This work deals with highly flexible laminated shell structures. The main focus is to provide an advanced model for the accurate prediction of the interlaminar three-dimensional (3D) stress state of shells subjected to large displacements/rotations, buckling and snap-through phenomena. In this context, a two-dimensional (2D) shell finite element based on the Carrera Unified Formulation (CUF) is formulated in an orthogonal curvilinear reference system. Thanks to CUF, the governing equations are expressed in terms of fundamental nuclei, which are invariant of the shell theory approximation order. Thus, classical theories of structures to layerwise approaches can be implemented with ease and in a unified manner. The full Green-Lagrange strain tensor is employed because far nonlinear regimes are investigated. Furthermore, the geometrical nonlinear equations are written in a total Lagrangian framework and solved with an opportune Newton-Raphson method along with a path-following approach based on the arc-length constraint. The results demonstrate that classical theories may bring to wrong and unconservative stress predictions, especially in nonlinear equilibrium states, where the use of advanced and layerwise approaches shall be recommended.**

## Nomenclature

|                      |   |   |
|----------------------|---|---|
| $\mathbf{b}$         | = | differential operator                   |
| $\tilde{\mathbf{C}}$ | = | matrix of material elastic coefficients |
| $F_\tau, F_s$        | = | thickness functions                     |
| $\mathbf{K}_S$       | = | secant stiffness matrix                 |

---

<sup>\*</sup>Associate professor. E-mail: alfonso.pagani@polito.it

<sup>†</sup>PhD student. E-mail: rodolfo.azzara@polito.it

<sup>‡</sup>PhD student. E-mail: riccardo.augello@polito.it

<sup>§</sup>Professor. E-mail: erasmus.carrera@polito.it

$\mathbf{K}_T$  = tangent stiffness matrix  
 $N_i, N_j$  = shape functions  
 $\mathbf{p}$  = loading vector  
 $\mathbf{q}$  = nodal unknowns  
 $R_\alpha, R_\beta$  = radii of curvature  
 $\mathbf{S}$  = second Piola-Kirchhoff stress vector  
 $\mathbf{u}$  = displacement vector  
 $\delta$  = virtual variation  
 $\boldsymbol{\epsilon}$  = Green-Lagrange strain vector

Subscripts

ext = external  
 int = internal  
 l = linear  
 nl = nonlinear

## I. Introduction

Thin-walled structures are increasingly employed in a large number of engineering applications, such as aerospace, marine, civil and automotive, among others. In particular, shells consist in curved lightweight constructions, and they turn out to be very popular in structural engineering mainly for their characteristic of supporting external loads with high efficiency. Their outstanding mechanical properties are due to the curvature, which generates coupling between the membrane and the flexural behaviour, in both single and doubly curved geometries. Furthermore, shell models are capable of undergoing large displacements and rotations when external loadings conditions become extreme. For the same reason, the assumptions of linear geometrical relations hold for a narrow range of applications. Indeed, thin shells exhibit large rotations even for moderate loadings and, therefore, geometrical nonlinear relations must be generally considered [1].

The literature about theories of shells constructions is vast [2–5]. This topic was developed in many research works to obtain efficient shell formulations to perform static and dynamic analyses. Lately, considerable importance was focused on the development of accurate theories to implement the effects of shear deformation and normal transverse stress in composite shells. The classical formulations are represented in literature from the studies by Poisson [6], Love [7], Mindlin [8], Kirchhoff [9], Reissner [10] and Cauchy [11]. Commercial codes adopt these classical theories in their two-dimensional (2D) elements. Recently, different higher-order 2D formulations were implemented to overcome the assumptions made in classical studies. These improvements become fundamental when composite structures are

analyzed, and whenever the through-the-thickness stresses need to be evaluated with a reliable accuracy.

As reported by Kapania [12], shell structures made of composite material are having a crucial use in different branches of engineering, in particular in aerospace. Composite materials provide an attractive possibility to more traditional construction types thanks to its resistance to corrosion, high strength-to-weight ratio, ease of formability, excellent fatigue strength, and tailoring ability. However, the study of the behaviour of laminated models is not a simple task because of the anisotropy nature of the material, and it turns to be a challenging issue for scientists and researchers. A large number of higher-order shell theories were developed in history, and many of those are presented here. Reddy [13] provided a refined through-the-thickness kinematic, including a higher-order shear deformation to study composite shell structures. The same author reported the mechanics of laminated plate and shell structures in [14]. A refined shear-deformation model based on finite-rotations formulation with seven independent displacement variables to study arbitrary multilayered composite shells was implemented by Bařar *et al.* [15]. Mashat *et al.* [16] provided an assessment of the relevance of displacement variables in refined theories for isotropic and multilayered shells using an axiomatic/asymptotic technique. A refined approach for analyzing the effect of shear deformation in thick laminated anisotropic shell structures was described by Jing and Tzeng [17]. Shu [18] performed different refined analyses to derive a refined formulation accounting for a higher-order transverse shear deformation to study composite shell structures. The refined theories of shell models were unified by Carrera in his early works, e.g., [19]. Cinefra and Carrera [20] provided several linear static analyses of composite structures adopting a finite shell model with different through-the-thickness kinematics. Petrolo and Carrera [21] developed a useful review of methods and guidelines for the selection of shell models. Other significant works on refined shell theories can be found in [22, 23].

In general, there are two main categories of theories for the study of the multilayered shells that differ from the through-the-thickness variables expansion: the Equivalent Single Layer (ESL) [24–26] and the Layerwise (LW) approaches [27, 28]. ESL formulations can be further divided into classical shell theories and high-order theories. According to the ESL approach, the variables of the theory do not depend on the number of layers and are considered over the entire thickness. Although this formulation simplifies the modelling and formulation procedure, they are only adequate for evaluating the global responses of thin laminated shells. Moreover, they lack the ability to accurately calculate the three-dimensional (3D) stress field, and to ensure the continuity of strain components between adjacent layers. On the other hand, in LW formulations, each layer is formulated independently from each other, and the interlaminar continuity is guaranteed. Compared to the former approach, the LW theory presents the drawback of a higher computational effort. A few examples of the adoption of these theories are reported hereafter, for completeness purpose. Reddy [29] reported an analysis of both theories for the investigation of composite laminates. An implementation of the LW mixed theory for laminated plates analysis was carried out by Carrera [30]. Li *et al.* [31] used the same approach combined with solid Finite Elements (FEs) for modelling the composite stiffened shell structure and the compatibility condition to satisfy the continuity of displacements at the interface. A LW method in the isogeometric scheme to study the 3D stress

distributions in composite structures was described by Guo *et al.* [32]. A review of LW theories for composite laminates was provided by Liew *et al.* [33]. A variable kinematics composite shell element was presented by Carrera *et al.* [34]. Zappino *et al.* [35] performed several analyses on laminated plates adopting Node-Dependent Kinematic (NDK) FEs employing both theories in a global-local sense. From the literature review, it can be understood that LW models are more accurate than ESL models in many cases. At the same time, LW theories are more expensive than ESL in terms of computational cost.

As reported by Liew *et al.* [33], laminated composite models show very complex behaviour if subjected to extreme external loads, which induce large rotations. In most of the studies, the solution is obtained through approximated computational methods [36, 37]. A large variety of studies has been performed on the nonlinear static and dynamic analysis of laminated shells. As an example, Han *et al.* [38] presented a 2D model with a shear distribution of a first-order type to perform geometrical nonlinear analyses of composite shell structures with large displacement field, but with the limit of validity only in the case of small strains. Amabili and Reddy [39] formulated a theory of first-order thickness stretching with higher-order shear strain using 6 independent parameters. All nonlinear terms are considered in the middle plane, while those relating to rotations and deformations are neglected. Amabili and Reddy [40] adopted a third-order thickness and shear deformation theory to perform both nonlinear static and dynamic analyses of doubly-curve composite shell structures. A new third-order thickness and shear deformation theory, including nonlinearities in rotation, by using 8 parameters was developed by Amabili [41]. This proposed theory, also considering geometric imperfections, was used to investigate laminated shells' static and dynamic behaviors. Rivera *et al.* [42] implemented a new 12 independent parameters shell FE using third-order thickness stretch kinematics to analyze large deflection of laminated shell structures. A detailed description of the nonlinear shell theories and more recent advances on these composite structures and their nonlinear vibrations was presented by Amabili [43]. The same author [44] discussed both the theoretical and experimental peculiarities of nonlinear vibrations and the stability of shells and plates. Boutagouga and Djeghaba [45] proposed an investigation on the proper FE to use in linear and nonlinear static and dynamic analyses. Moreover, the effects of the thickness on the geometrical nonlinear response of shells was investigated by Chaudhuri and Hsia [46] and by Chaudhuri and Kim [47, 48]. Kim and Chaudhuri [49] presented a fully nonlinear FE analysis for postbuckling response of moderately thick imperfect rings under external pressure. The same authors show as the additional terms also retained in the present nonlinear theory, but ignored by the von Kármán theory, play crucial roles, especially in the advanced nonlinear regime. A 3D shell element for nonlinear analyses of composites shell models was provided by Klinkel *et al.* [50]. A geometrical nonlinear shear deformation formulation for the laminated shell was presented by Dennis and Palazotto [51]. Sze *et al.* [52] suggested different nonlinear benchmark problems of shells. Librescu [53] proposed a nonlinear theory for anisotropic laminates shells.

The goal of this work is to accurately evaluate the 3D stress distributions of composite shells in the large displacement/rotation field. The proposed model has its foundations on the Carrera Unified Formulation (CUF). The

literature on the evaluation of the complete 3D stress field of laminated composite shells is limited. For this reason, this paper has the goal to present stress benchmarks for future comparisons. As previously reported, the nonlinear analysis proposed in the present manuscript is conducted in the domain of CUF. In CUF, any degree of refinement of a model can be obtained, since the order of the adopted theory is treated as an input of the analysis. CUF was used for the first time by Carrera [54]. It was adopted to obtain a class of 2D theories through a compact formulation, and it was then extended to multilayered, composite plates and shell [19], and later for beam modelling [55]. Basically, the nonlinear governing equations and the related FE arrays of any model is formulated by means of *fundamental nuclei* (FN). By an opportune expansion of the FNs, any order of theory can be achieved. The expansions functions and their order over the thickness direction can be an arbitrary choice. In the present research, both ESL models using Taylor expansions (TE) and LW models adopting the Lagrange expansion (LE) are employed. Furthermore, note that the nonlinear procedure adopted is an extension of the works of Pagani and Carrera [56] and Wu et al. [57].

This paper is structured as follows: (i) firstly, preliminary information about the 2D CUF model is illustrated in Section II, including the Green-Lagrange nonlinear geometrical relations and a brief description of the two modelling approaches used; (ii) then, in Section III the method used to perform geometrical nonlinear analyses is described; Finally, in Section IV the numerical results considering the proposed CUF shell model are presented, and the conclusions are reported in Section V.

## II. Unified finite shell element

### A. Preliminaries

A shell is a 2D structural element which thickness is negligible compared to the other dimensions. Let us suppose a curvilinear reference system as depicted in Fig. 1, where  $\alpha$  and  $\beta$  are the coordinates of the shell surface and, as a consequence,  $z$  lays along the thickness  $h$  direction.

Considering a multilayered shell structure in an orthogonal coordinate system, the square of an infinitesimal linear segment in the layer  $ds_k^2$ , the associate in-plane area  $d\Omega_k$  and volume  $dV$  can be expressed as:

$$ds_k^2 = H_\alpha^{k^2} d\alpha_k^2 + H_\beta^{k^2} d\beta_k^2 + H_z^{k^2} dz_k^2$$

$$d\Omega_k = H_\alpha^k H_\beta^k d\alpha_k d\beta_k \tag{1}$$

$$dV = H_\alpha^k H_\beta^k H_z^k d\alpha_k d\beta_k dz_k$$

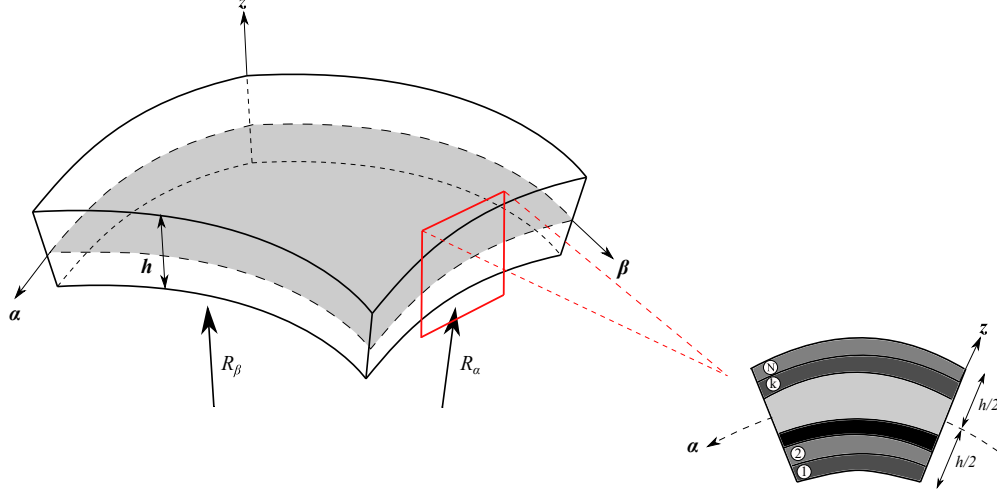


**Fig. 1** Geometry and reference system of a generic laminated doubly-curved shell.

where and  $H_\alpha^k$ ,  $H_\beta^k$  and  $H_z^k$  are:

$$H_\alpha^k = A^k (1 + z_k/R_\alpha^k), \quad H_\beta^k = B^k (1 + z_k/R_\beta^k), \quad H_z^k = 1 \quad (2)$$

In Eq. (2)  $k$  indicates the  $k$ -layer of the laminated shell,  $R_\alpha^k$  and  $R_\beta^k$  represent the radii of the middle surface of the layer  $k$ ,  $A^k$  and  $B^k$  are the coefficients related to  $\Omega_k$ . This paper considers only shells with constant curvatures, therefore  $A^k = B^k = 1$ . The complete description of the shell formulation is not the purpose of this article, and more details can be found in [14, 57, 58]. Also, note that geodesic curvature, which is important for modelling boundaries of doubly curved panels and singly curved ones with cut-outs [59], is not considered in this work.

As far as the strain and stress definitions are concerned, the present study makes use of a total Lagrangian approach ([60]). The advantage of using this formulation is that strains are formulated with respect to the the undeformed configuration. In this domain, the Green-Lagrange strains  $\epsilon$ , and the Second Piola-Kirchhoff (PK2) stresses  $S$  are considered. The strain and stress components for each layer  $k$  can be written, with respect of the curvilinear system, in vectorial form as follows:

$$\epsilon^k = \{\epsilon_{\alpha\alpha}^k, \epsilon_{\beta\beta}^k, \epsilon_{zz}^k, \epsilon_{\alpha z}^k, \epsilon_{\beta z}^k, \epsilon_{\alpha\beta}^k\}^T \quad (3)$$

$$S^k = \{S_{\alpha\alpha}^k, S_{\beta\beta}^k, S_{zz}^k, S_{\alpha z}^k, S_{\beta z}^k, S_{\alpha\beta}^k\}^T$$

The strain vector  $\epsilon^k$  is obtained via the displacement-strain relations:

$$\epsilon^k = \epsilon_l^k + \epsilon_{nl}^k = (\mathbf{b}_l + \mathbf{b}_{nl})\mathbf{u}^k \quad (4)$$

where  $\mathbf{b}_l$  and  $\mathbf{b}_{nl}$  represent the linear and nonlinear differential operators. These differential operators in the case of 2D models are reported in [61]. The stresses are computed from the constitutive equations as follows:

$$\mathbf{S}^k = \tilde{\mathbf{C}}^k \boldsymbol{\epsilon}^k \quad (5)$$

where  $\tilde{\mathbf{C}}$  is the material elastic matrix ([62, 63]).

### B. Carrera Unified Formulation (CUF)

In the literature, classical shell models provide reliable results for 2D homogeneous structures with thin thickness. In contrast, when dealing with multilayered structures with thick thickness, more sophisticated formulations are needed to obtain accurate results. In CUF domain, the refinement of the adopted theory is considered as an input of the analysis, so low- to higher-order models can be built with ease and in a unified manner (i.e. no ad-hoc formulation are needed to obtain any model). Basically, the 3D displacement field  $\mathbf{u}(\alpha, \beta, z)$  of a generic shell structure can be written as an arbitrary through-the-thickness (along  $z$ ) expansion of the in-plane ( $\alpha$  and  $\beta$ ) variables.

$$\mathbf{u}^k(\alpha, \beta, z) = F_\tau^k(z) \mathbf{u}_\tau^k(\alpha, \beta) \quad \tau = 0, 1, \dots, N \quad (6)$$

where  $\mathbf{u}_\tau(\alpha, \beta)$  indicates the generalized in-plane displacement vector,  $F_\tau$  represents the through-the-thickness expansion functions along coordinate  $z$ ,  $\tau$  is the dummy index over which summation is carried out,  $k$  indicates the layer index in laminated shells and  $N$  is the order of expansion. Readers are referred to [64] for further information about the derivation of the shell FE formulations within CUF domain.

### C. Modelling approaches

As previously reported, laminated composite structures lead to important challenges in the design process. Nevertheless, these particular structures exhibit complex behaviour when subjected to external loads. Then, it is essential to evaluate the stress and strain distributions correctly in composite structures. In the literature, ESL and LW theories are typically adopted when dealing with composite materials. The selection of the modelling approaches is independent of the polynomials adopted. Considering the ESL approach, the stiffness matrix is evaluated with the homogenization technique of the properties of each layer by summing the contributions of each layer. Moreover, it allows obtaining a model that considers a set of variables independent of the number of layers. The  $F_\tau$  of the ESL technique are reported in the following:

$$F_0 = z^0 = 1, \quad F_1 = z^1 = z, \quad F_N = z^N \quad (7)$$



where  $N$  denotes the number of terms of the through-the-thickness expansion. ESL theories exhibit accurate results of the global response (fundamental vibration frequency, transverse deflection), but they are often inaccurate for the 3D stress distributions evaluation. For illustrative purposes, Fig. 2a shows the general behaviour of the primary variables in the thickness direction of the shell.

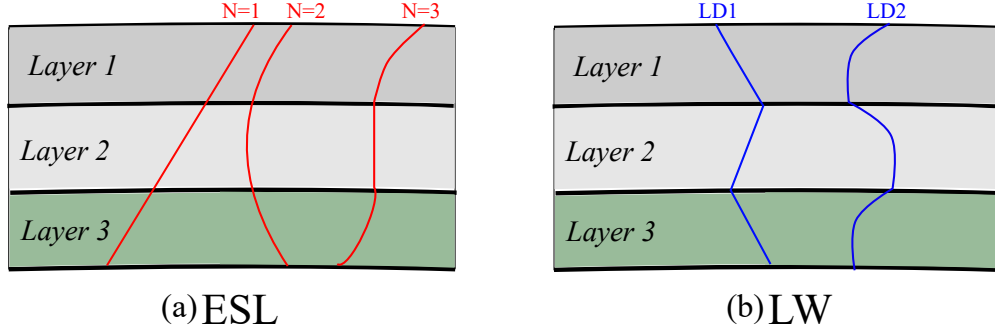


**Fig. 2** ESL (a) and LW (b) behaviour of the primary variables along the thickness of the shell.

On the contrary to the ESL approach, LW theories divide and expand the displacement field within each material layer. The continuity of displacements is guaranteed at the interface level, to have an accurate evaluation of the deformation and stress distributions. By doing so, the homogenization is carried out at the interface layer. By adopting LE in LW models, the displacements on each interpolation are assumed as unknowns, and displacements at each interface obey the compatibility conditions, as shown in Fig. 2b, where the adopted shell formulations are denoted by the acronym  $LDN$ , which represent the LE of order  $N$ . In particular, the two-node linear (LD1), three-node quadratic (LD2), and the four-node cubic (LD3) Lagrange expansion functions are assumed in the thickness direction in order to generate linear to higher-order kinematics CUF shell models. Independently of the selected shell model kinematics, the finite element method is adopted to discretize the in-plane generalized displacement vector, as follows:

$$\mathbf{u}_{\tau}^k(\alpha, \beta) = N_i(\alpha, \beta) \mathbf{q}_{\tau i}^k \quad i = 1, 2, \dots, n_{el} \quad (8)$$

where  $N_i(\alpha, \beta)$  are the shape functions,  $\mathbf{q}_{\tau i}$  represents the unknown nodal variables,  $n_{el}$  is the number of nodes per element and the  $i$  indicates summation. In the following analyses, the classical 2D nine-node quadratic (Q9) FE will be considered as the shape function. For the sake of completeness, Fig. 3 shows the approximations for a typical shell structure, with the difference between an ESL and LW approach.

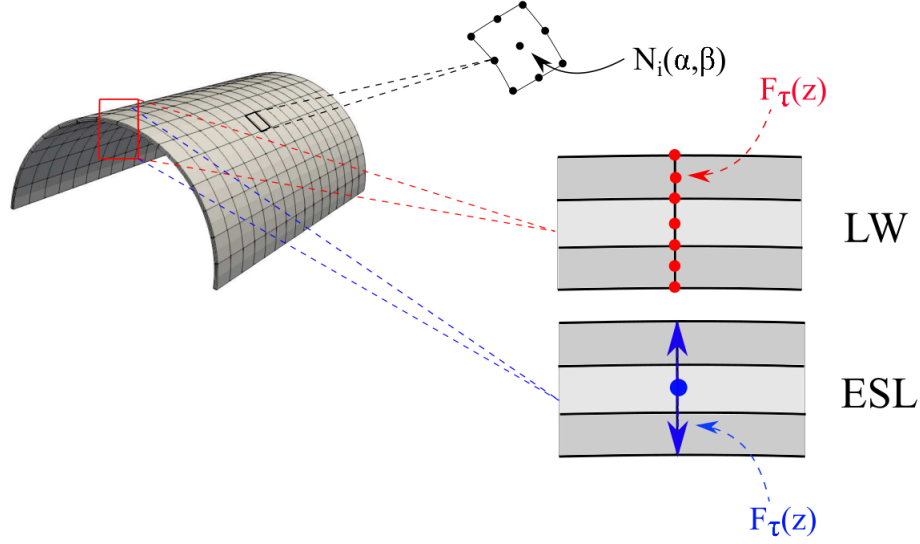


**Fig. 3 FE discretization and ESL/LW approaches in the modelling of shells.**

### III. Nonlinear governing equations and related FE approximation

When large displacements and rotation occur within the structure, nonlinear analyses are necessary. For the formulation of the nonlinear FE equations, the principle of virtual work is used. Hence:

$$\delta L_{int} = \delta L_{ext} \quad (9)$$

where  $\delta L_{int}$  and  $\delta L_{ext}$  are the virtual variation of the strain energy and the virtual variation of the work of external loadings, respectively. After some mathematical steps, which are not reported here, but that can be found in [56], the nonlinear equilibrium conditions and the related finite element arrays of the generic shell model are formulated as follows:

$$\mathbf{K}_S^{ij\tau s} \mathbf{q}_{\tau i} - \mathbf{p}_{sj} = 0 \quad (10)$$

which is a set of three nonlinear algebraic equations, where  $\mathbf{K}_S^{ij\tau s}$  is the *secant* stiffness matrix and  $\mathbf{p}_{sj}$  represents the nodal loading vector. Note that  $\mathbf{K}_S^{ij\tau s}$  is expressed by means of *fundamental nuclei*, which are  $3 \times 3$  matrices that can be expanded by using the indexes  $i, j, \tau$  and  $s$ . The complete form of  $\mathbf{K}_S^{ij\tau s}$  and  $\mathbf{p}_{sj}$  is omitted here, see [56, 65] for its derivation.

For the resolution of the nonlinear system, an iterative method is needed. In this work, an incremental linearized scheme, the Newton-Raphson method [66–68] along with a path-following approach based on the arc-length constraint, is adopted to compute the geometrical nonlinear systems. Consequently, the so-called tangent stiffness matrix  $\mathbf{K}_T = \frac{d(\mathbf{K}_S \mathbf{q} - \mathbf{p})}{d\mathbf{q}}$  is introduced. The explicit form of  $\mathbf{K}_T$  is not given here, but it is derived in a unified form in [56]. The complete formulation and related mathematical passages are not the scopes of this article and the reader is referred to [69] for a

complete description. In the present work, the main attention is directed to the evaluation of the 3D stress distributions in the thickness direction and to provide stress benchmark problems for geometric nonlinear analysis of shells. Different shell structures, constraints and loadings are considered.

## IV. Numerical results

This section discusses representative benchmark problems, and particular emphasis is given to the capabilities of the proposed geometrical nonlinear approach to deal with 3D stress fields. Laminated composite shell structures are analyzed. Both ESL and LW approaches are adopted and compared in a total Lagrangian scenario. In order to perform several analyses to investigate the stress accuracy, different 2D CUF shell models are employed in the static analyses. In particular, LD1, LD2, LD3 and TE functions are used in the numerical investigations. First, convergence analyses are shown and, then, on the converged model, PK2 stresses are evaluated. The considered cases are inspired by Sze's well-known paper [52].

### A. Pinched composite cylindrical shell

A clamped composite cylindrical shell subjected to a pinching force is considered as first analysis case. The vertical displacement and the rotation around the  $\beta$ -axis are constrained along its longitudinal edges. The laminated cylindrical shell model, considering stacking sequences  $[90^\circ, 0^\circ, 90^\circ]$  and  $[45^\circ, 0^\circ, -45^\circ]$ , is reported in Fig. 4. The investigated

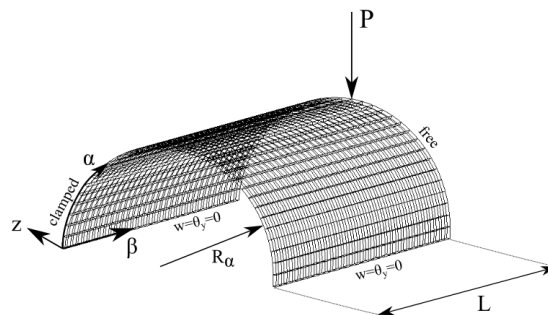


**Fig. 4 Pinched cylindrical shell subjected to an end pinching force.**

model has the following characteristics:  $L= 3.048$  m,  $R_\alpha= 1.016$  m, and  $h=0.03$  m. The material has an elastic modulus  $E_L= 2068.5 \times 10^4$  N/m<sup>2</sup>,  $E_T= 517.125 \times 10^4$  N/m<sup>2</sup>,  $G_{LT}= 795.6 \times 10^4$  N/m<sup>2</sup> and Poisson's ratio  $\nu_{LT}=\nu_{TT}= 0.3$ . The subscripts  $L$  and  $T$  indicate the longitudinal and transverse (fiber) direction, respectively. This static analysis case was presented by Wu *et al.* [57] and by Sze *et al.* [52]. Nevertheless, no through-the-thickness stress benchmarks were yet described. In this article, a stress benchmark for the pinched composite cylindrical shell is provided as an addition to the literature.

First, in order to perform an accurate static analysis, a convergence study on the in-plane finite element mesh is carried out. Figure 5 shows the transverse deflection at the load point for different 2D shell models, and from 256Q9 to

1024Q9 FEs are adopted for the surface approximation, whereas one LD2 is used in each layer in the thickness direction. Moreover, Table 1 shows the transverse displacement values for different models and loads, along with the total degrees

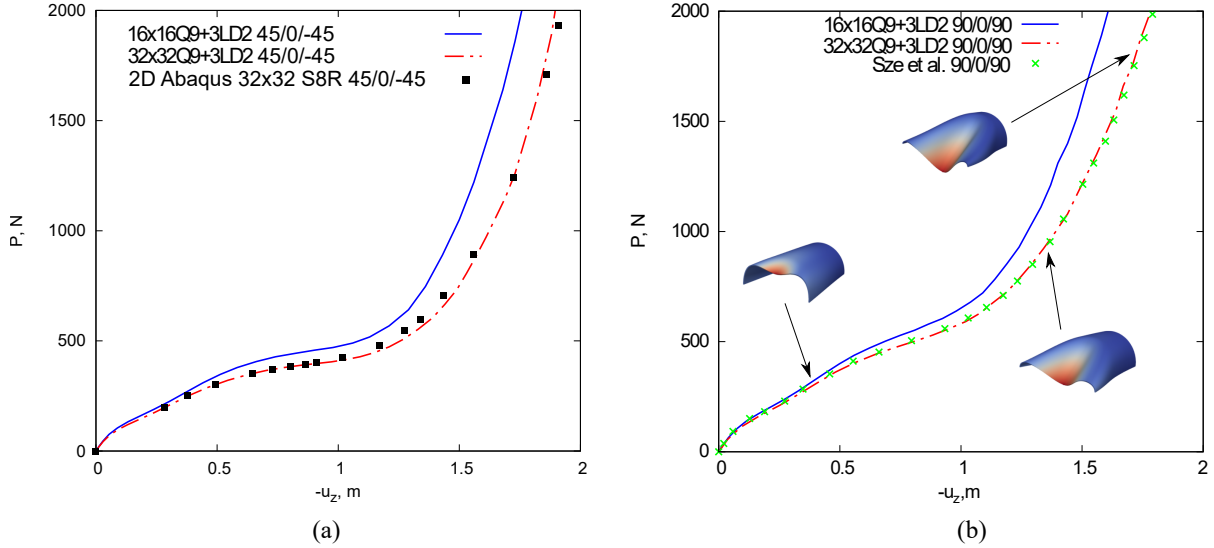


**Fig. 5** Convergence analysis of nonlinear response curves for the pinched cylindrical shell at the load point. Comparison of different in-plane mesh approximations. Lamination sequence: (a)  $[45^\circ, 0^\circ, -45^\circ]$ , (b)  $[90^\circ, 0^\circ, 90^\circ]$ .

of freedom (DOFs). As evident from Fig. 5 and Table 1, the 32x32Q9 mesh is a reliable approximation for the

**Table 1** Equilibrium points of nonlinear response curves of the pinched cylindrical shell for different in-plane mesh approximations and loads at  $\alpha = 1.596$  m,  $\beta = 3.048$  m and  $z = 0.015$  m.

| Model                  | DOFs  | $-u_z$ [m]                       |        |                                 |        |
|------------------------|-------|----------------------------------|--------|---------------------------------|--------|
|                        |       | $[45^\circ, 0^\circ, -45^\circ]$ |        | $[90^\circ, 0^\circ, 90^\circ]$ |        |
|                        |       | 500 N                            | 1000 N | 500 N                           | 1000 N |
| 16 x 16Q9 + 3LD2       | 22869 | 1.086                            | 1.481  | 0.684                           | 1.273  |
| 32 x 32Q9 + 3LD2       | 88725 | 1.267                            | 1.632  | 0.807                           | 1.394  |
| Sze <i>et al.</i> [52] | -     | -                                | -      | 0.798                           | 1.393  |

in-plane description. Then, to perform an accurate stress prediction, different expansion functions in the thickness direction are compared. Both LE and TE functions are considered in this analysis. Figure 6 shows the 3D stress distributions, including the circumferential normal stress  $S_{\alpha\alpha}$  and the transverse shear stress  $S_{\beta z}$  components, for different through-the-thickness kinematic approximations. The corresponding stress values are reported in Table 2 for different 2D shell theories and loads. Clearly, the LW model kinematics should be exploited to accurately predict the stress values, using at least the 3LD3 theory. The results suggest that the ESL model is sufficient to evaluate the circumferential normal stress, whereas it is inadequate to accurately predict the transverse shear stress component. Moreover, about the transverse shear distribution, TE3 and TE4 show a similar distribution compared to the most

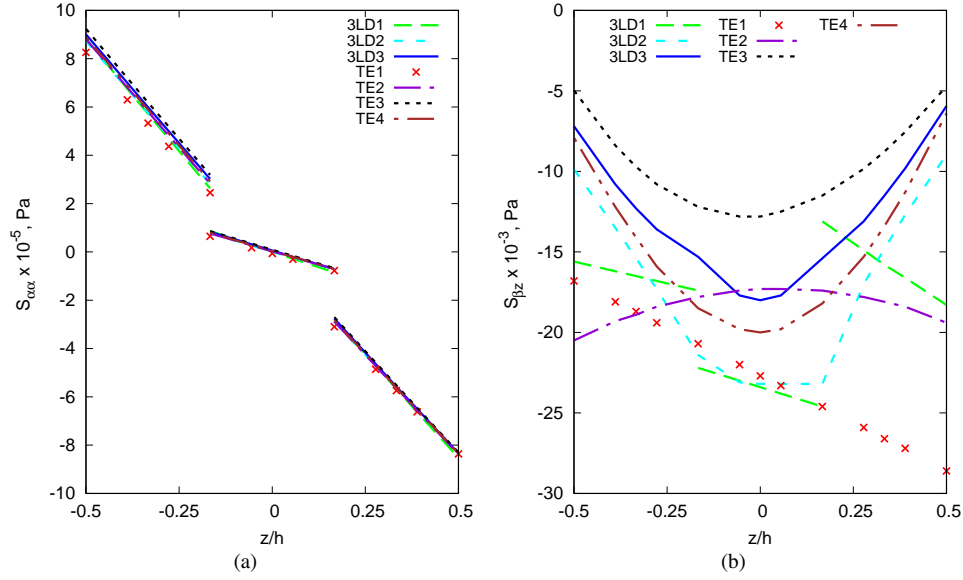


**Fig. 6** Convergence analysis of the pinched cylindrical shell under a point load,  $P=1000$  N, for stresses evaluation at  $\alpha=1.596$  m and  $\beta=1.524$  m. Comparison of various orders of both Lagrange expansion functions in the thickness direction and Taylor expansions.  $32 \times 32 \times 9$  in-plane mesh model. Lamination sequence  $[90^\circ, 0^\circ, 90^\circ]$ .

**Table 2** Circumferential normal stress and transverse shear stress values of nonlinear response curves of the pinched cylindrical shell (with  $32 \times 32 \times 9$  in-plane mesh) for different theories and loads at  $\alpha=1.596$  m and  $\beta=1.524$  m and  $z=0.015$  m  $S_{\alpha\alpha}$  and  $z=0$  m for  $S_{\beta z}$ .

| Theory | DOFs   | [90°, 0°, -90°]                        |        |                                   |         |
|--------|--------|--|--------|-----------------------------------|---------|
|        |        | $S_{\alpha\alpha}$ [Pa $\times 10^5$ ] |        | $S_{\beta z}$ [Pa $\times 10^3$ ] |         |
|        |        | 500 N                                  | 1000 N | 500 N                             | 1000 N  |
| TE1    | 25350  | -1.280                                 | -8.356 | -1.151                            | -22.658 |
| TE2    | 38025  | -1.291                                 | -8.375 | -1.110                            | -17.291 |
| TE3    | 50700  | -1.272                                 | -8.298 | -1.573                            | -12.760 |
| TE4    | 63375  | -1.282                                 | -8.344 | -1.657                            | -19.973 |
| 3LD1   | 50700  | -1.309                                 | -8.519 | -1.622                            | -23.399 |
| 3LD2   | 88725  | -1.289                                 | -8.350 | -1.600                            | -23.185 |
| 3LD3   | 126750 | -1.289                                 | -8.350 | -1.776                            | -18.001 |

accurate LD3. This aspect underlines the needs to take into account the cubic terms of the thickness expansion for an accurate evaluation of the this through-the-thickness stress component. Figures 7 and 8 depict the circumferential normal and transverse shear PK2 stresses in the thickness direction for different loads and for the two laminations using both ESL and LW approaches to highlight the different capabilities. The linear interpolation (*FSDT-like*) provided

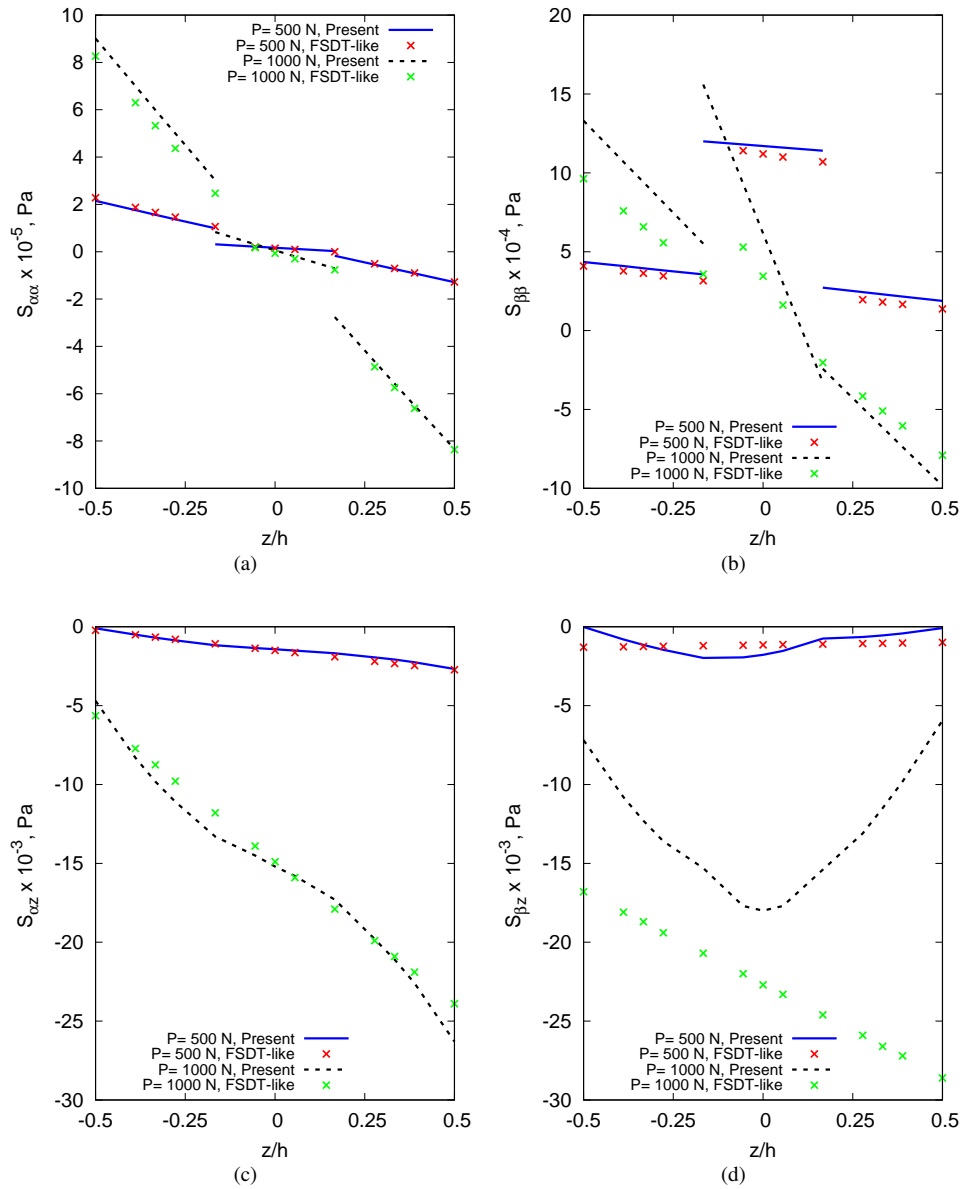


**Fig. 7** Through-the-thickness distribution of stresses for different loads at  $\alpha = 1.596$  m and  $\beta = 1.524$  m. Pinched cylindrical shell with  $32 \times 32 Q9$  model. Lamination sequence  $[90^\circ, 0^\circ, 90^\circ]$ .

by the ESL model is, clearly, not enough to catch the transverse shear stress distribution of the laminated pinched cylindrical shell, as shown in Figs. 7d and 8d.

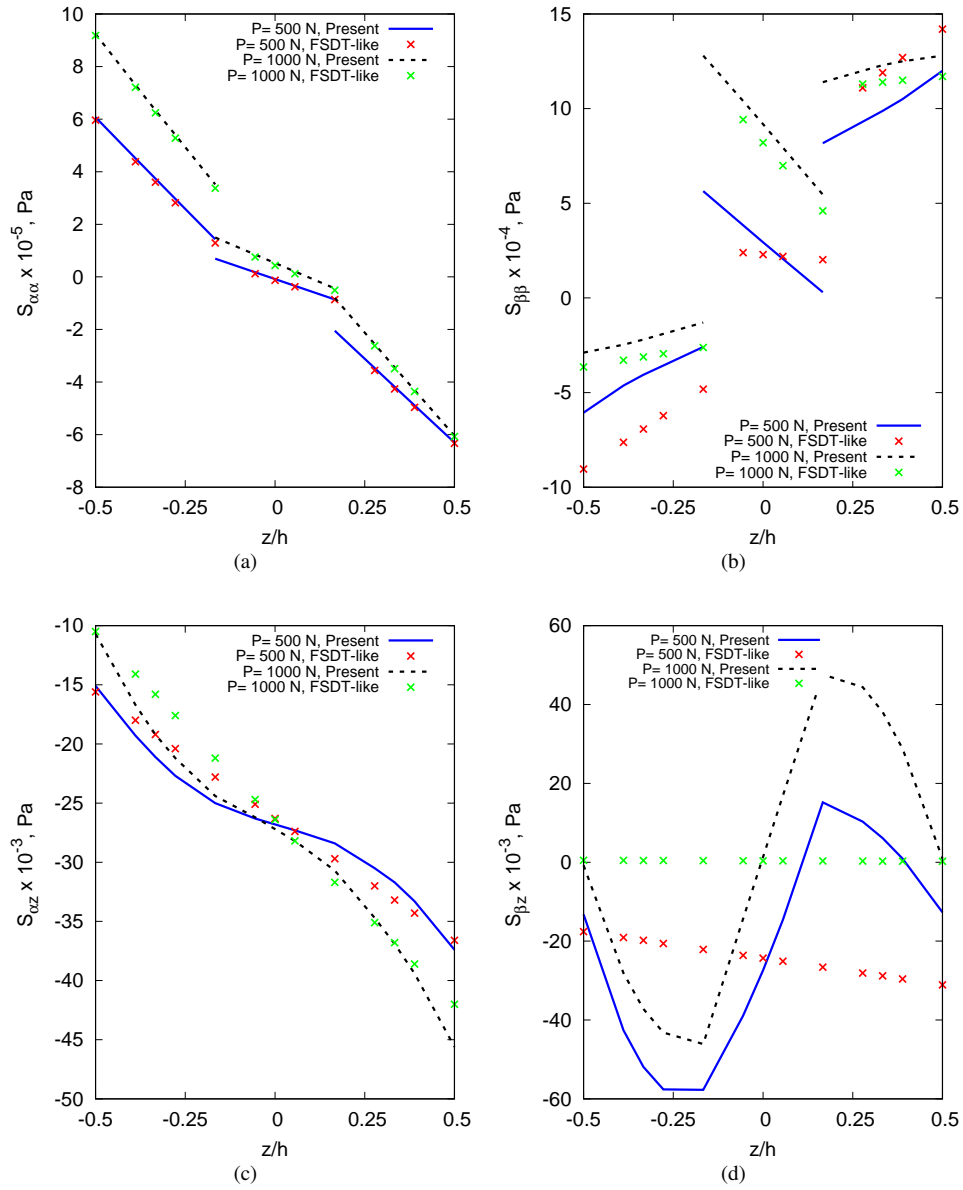


**Fig. 8** Through-the-thickness distribution of stresses for different loads at  $\alpha = 1.596$  m and  $\beta = 1.524$  m. Pinched cylindrical shell with  $32 \times 32 Q9$  model. Lamination sequence  $[45^\circ, 0^\circ, -45^\circ]$ .

## B. Hinged composite cylindrical shell

As a second assessment, a hinged composite cylindrical shell under a central transverse force  $P$  is considered, as illustrated in Fig. 9. This is a well-known nonlinear benchmark and especially popular for the snapping behaviour. The

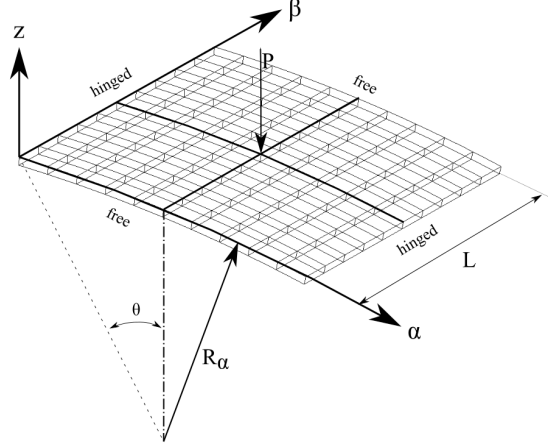


**Fig. 9 Hinged cylindrical shell under a central transverse force.**

present model has the following geometrical characteristics,  $L= 508$  mm,  $R_\alpha= 2540$  mm,  $\theta= 0.1$  rad. The material properties of the laminated hinged cylindrical shell involves  $E_L= 3300$  MPa,  $E_T= 1100$  MPa,  $G_{LT}= 660$  MPa,  $G_{TT}= 660$  MPa and  $\nu_{LT}=\nu_{TT}= 0.25$ . The lamination sequence considered are  $[0^\circ, 90^\circ, 0^\circ]$ ,  $[90^\circ, 0^\circ, 90^\circ]$  and  $[45^\circ, 0^\circ, -45^\circ]$ , and the thickness equals 12.7 mm.

First, in order to perform an accurate static analysis, a convergence study on the in-plane 2D shell model is carried out. Then, a stress evaluation is performed for different expansion orders. Figure 10 plots the transverse deflection for different in-plane FE mesh, and the elements from 25Q9 to 225Q9 are used for the surface discretization, whereas only one LD2 is adopted in each layer in the thickness direction. The nonlinear response curves are divided into the regions A, B and C, as reported in Fig. 10c. In addition, transverse displacements values for the three laminations for different in-plane mesh and loads are illustrated in Table 3, along with the number of DOFs. Consequently, the

**Table 3 Equilibrium points of nonlinear response curves of the hinged composite cylindrical shell for different in-plane mesh approximations and loads at  $\alpha= 254.0$  mm,  $\beta= 254.0$  mm and  $z= 6.35$  mm.**

| Model                  | DOFs  | $-u_z$ [mm]                    |           |           |        |                                 |        |                                  |           |           |        |
|------------------------|-------|--------------------------------|-----------|-----------|--------|---------------------------------|--------|----------------------------------|-----------|-----------|--------|
|                        |       | $[0^\circ, 90^\circ, 0^\circ]$ |           |           |        | $[90^\circ, 0^\circ, 90^\circ]$ |        | $[45^\circ, 0^\circ, -45^\circ]$ |           |           |        |
|                        |       | 500 N (A)                      | 500 N (B) | 500 N (C) | 2000 N | 500 N                           | 2000 N | 500 N (A)                        | 500 N (B) | 500 N (C) | 2000 N |
| 5 x 5Q9 + 3LD2         | 2541  | 2.521                          | 14.629    | 24.601    | 29.821 | 2.125                           | 27.069 | 2.620                            | 18.074    | 22.097    | 29.296 |
| 10 x 10Q9 + 3LD2       | 9261  | 2.701                          | 15.698    | 25.092    | 30.492 | 2.062                           | 27.701 | 2.879                            | 17.296    | 22.691    | 30.220 |
| 15 x 15Q9 + 3LD2       | 20181 | 2.702                          | 15.700    | 25.092    | 30.495 | 2.066                           | 27.709 | 2.883                            | 17.307    | 22.706    | 30.221 |
| Sze <i>et al.</i> [52] | -     | 2.697                          | 15.727    | 25.124    | 30.506 | 2.061                           | 27.722 | -                                | -         | -         | -      |

10x10Q9 mesh will be taken as converged discretization and, therefore, it is used for the following stress evaluation.



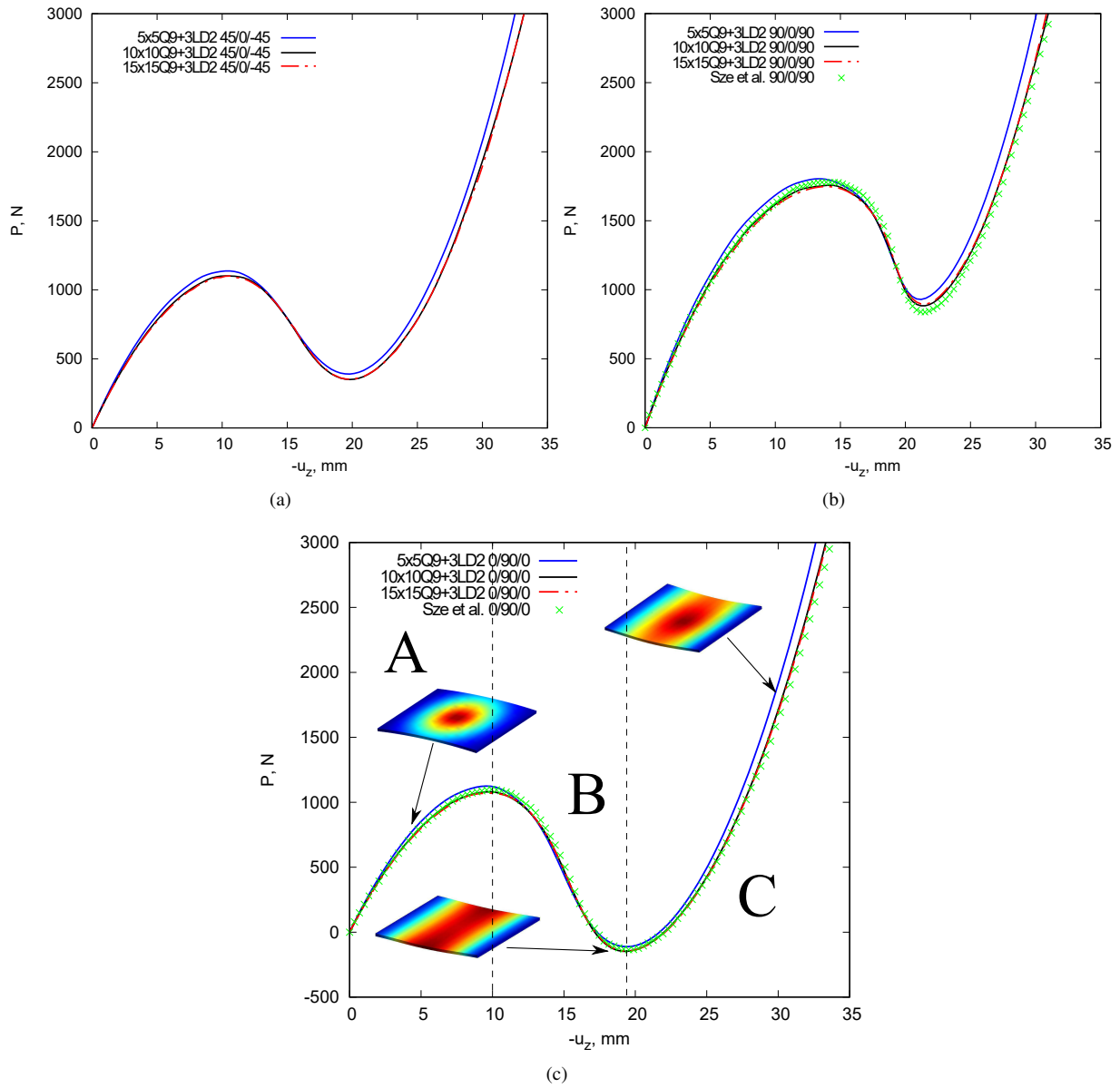


**Fig. 10** Convergence analysis of nonlinear response curves for the hinged cylindrical shell subjected to the transverse load. Comparison of different in-plane mesh numbers. Laminations sequence: (a)  $[45^\circ, 0^\circ, -45^\circ]$ , (b)  $[90^\circ, 0^\circ, 90^\circ]$ , (c)  $[0^\circ, 90^\circ, 0^\circ]$ .

Then, to perform an accurate stress prediction, both ESL and LW models are adopted and compared using different expansion functions in the thickness direction. Figure 11 shows the comparison for different kinematic theories for the stress assessment. The corresponding stress values are reported in Table 4 for different shell theories. Clearly, the LW

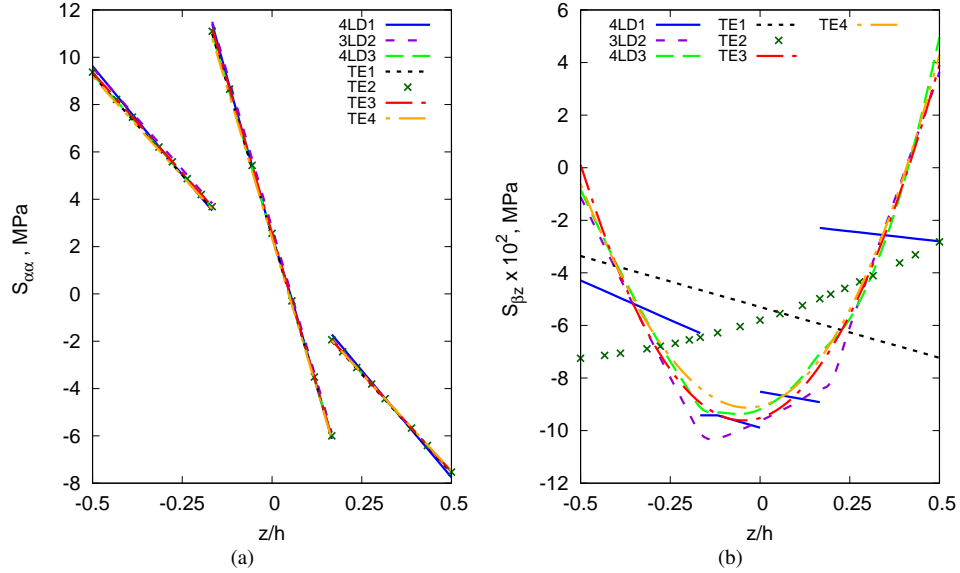


**Fig. 11** Convergence analysis of the hinged cylindrical shell under a point load,  $P=2000$  N, for stresses evaluation at  $\alpha=254.0$  mm and  $\beta=127.0$  mm. Comparison of various orders of both Lagrange expansion functions in the thickness direction and Taylor expansions.  $10 \times 10 \times 9$  in-plane mesh model. Lamination sequence  $[0^\circ, 90^\circ, 0^\circ]$ .

**Table 4** Circumferential normal stress and transverse shear stress values of nonlinear response curves of the hinged cylindrical shell (with  $10 \times 10 \times 9$  in-plane mesh) for different theories and loads at  $\alpha=254.0$  mm,  $\beta=127.0$  mm and  $z=6.35$  mm for  $S_{\alpha\alpha}$  and  $z=0$  mm for  $S_{\beta z}$ .

| Theory | DOFs  | $[0^\circ, 90^\circ, 0^\circ]$ |                                       | $[90^\circ, 0^\circ, 90^\circ]$ |                                       | $[45^\circ, 0^\circ, -45^\circ]$ |                                       |
|--------|-------|--------------------------------|---------------------------------------|---------------------------------|---------------------------------------|----------------------------------|---------------------------------------|
|        |       | $S_{\alpha\alpha}$ [MPa]       | $S_{\beta z}$ [MPa $\times 10^{-2}$ ] | $S_{\alpha\alpha}$ [MPa]        | $S_{\beta z}$ [MPa $\times 10^{-2}$ ] | $S_{\alpha\alpha}$ [MPa]         | $S_{\beta z}$ [MPa $\times 10^{-2}$ ] |
|        |       | 2000 N                         | 2000 N                                | 2000 N                          | 2000 N                                | 1500 N                           | 1500 N                                |
| TE1    | 2646  | -7.563                         | -5.299                                | -21.264                         | -2.135                                | -11.840                          | -3.360                                |
| TE2    | 3969  | -7.533                         | -5.802                                | -21.301                         | -2.530                                | -11.817                          | -3.607                                |
| TE3    | 5292  | -7.510                         | -9.518                                | -21.214                         | -4.211                                | -11.796                          | -5.919                                |
| TE4    | 6615  | -7.480                         | -9.069                                | -21.215                         | -4.231                                | -11.172                          | -6.260                                |
| 4LD1   | 6615  | -7.749                         | -9.899                                | -21.470                         | -3.861                                | -12.072                          | -5.932                                |
| 3LD2   | 9261  | -7.545                         | -9.635                                | -21.218                         | -3.998                                | -11.857                          | -5.943                                |
| 4LD3   | 17199 | -7.05                          | -9.192                                | -21.220                         | -4.157                                | -11.792                          | -5.949                                |

model should be exploited to accurately predict the stress values. Results suggest that the ESL model with a low-order model is sufficient to evaluate the circumferential normal stress, whereas it is inaccurate to predict the transverse shear stress component. Figures 12, 13 and 14 depict the circumferential normal and transverse shear stresses in the thickness

direction for different loads for the three laminations. As previously reported, the stresses obtained using both ESL and

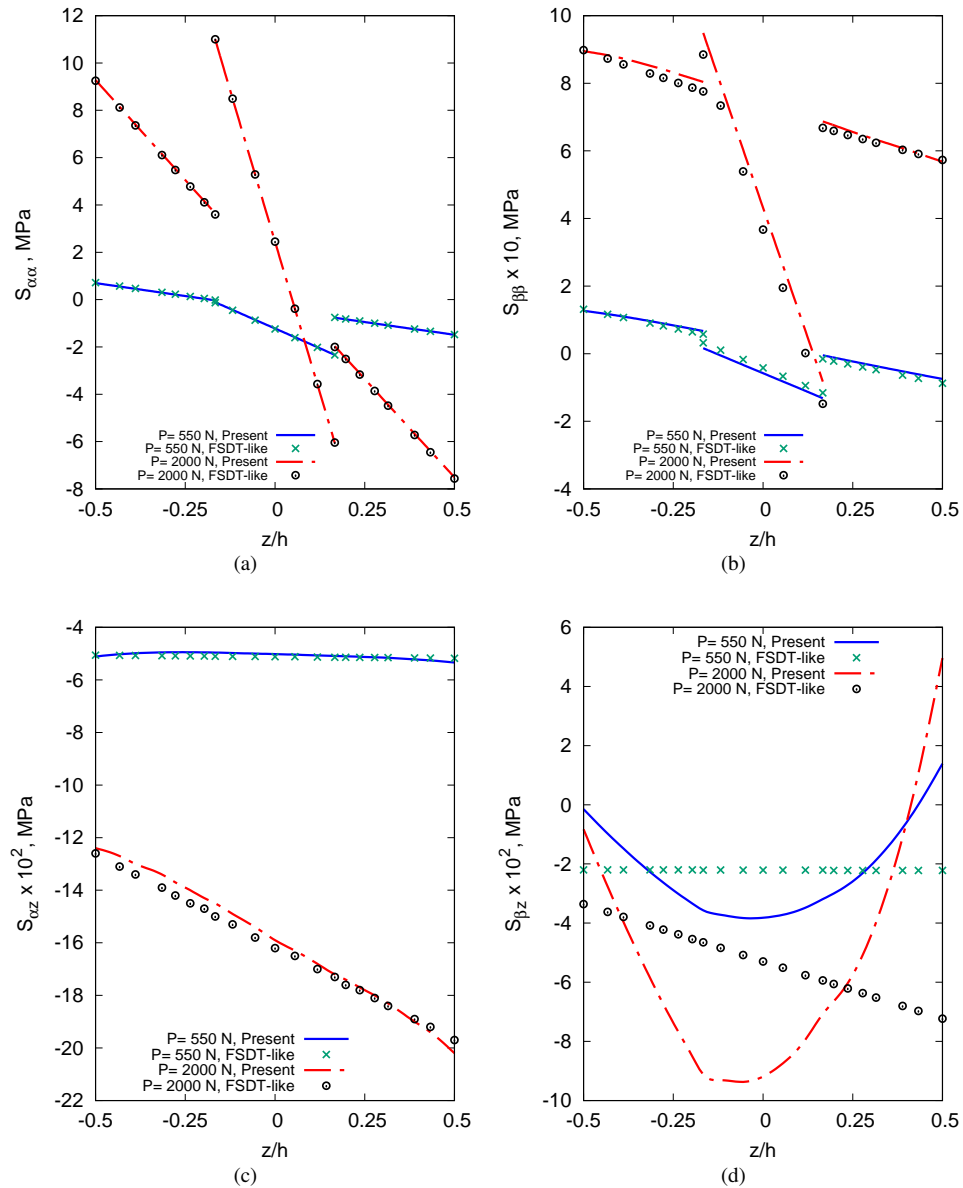


**Fig. 12** Through-the-thickness distribution of stresses for different loads at  $\alpha = 254.0$  mm and  $\beta = 127.0$  mm of the hinged cylindrical shell with  $10 \times 10Q9$  model. Lamination sequence  $[0^\circ, 90^\circ, 0^\circ]$ .

LW models with 4LD3 are plotted to show the different capabilities of the two approaches. According to Fig. 12d, ESL models are not able to accurately evaluate the transverse shear stresses.

In addition, another stress analysis is performed considering the hinged cylindrical shell with stacking sequence  $[90^\circ, 0^\circ, 90^\circ]$  subjected to a line force in  $\alpha = 254.0$  mm,  $z = 6.35$  mm. Figure 15 plots the equilibrium curve of the hinged cylindrical shell subjected to the line force. Furthermore, Fig. 16 illustrates the circumferential normal and transverse shear stresses in the thickness direction for the line load conditions.

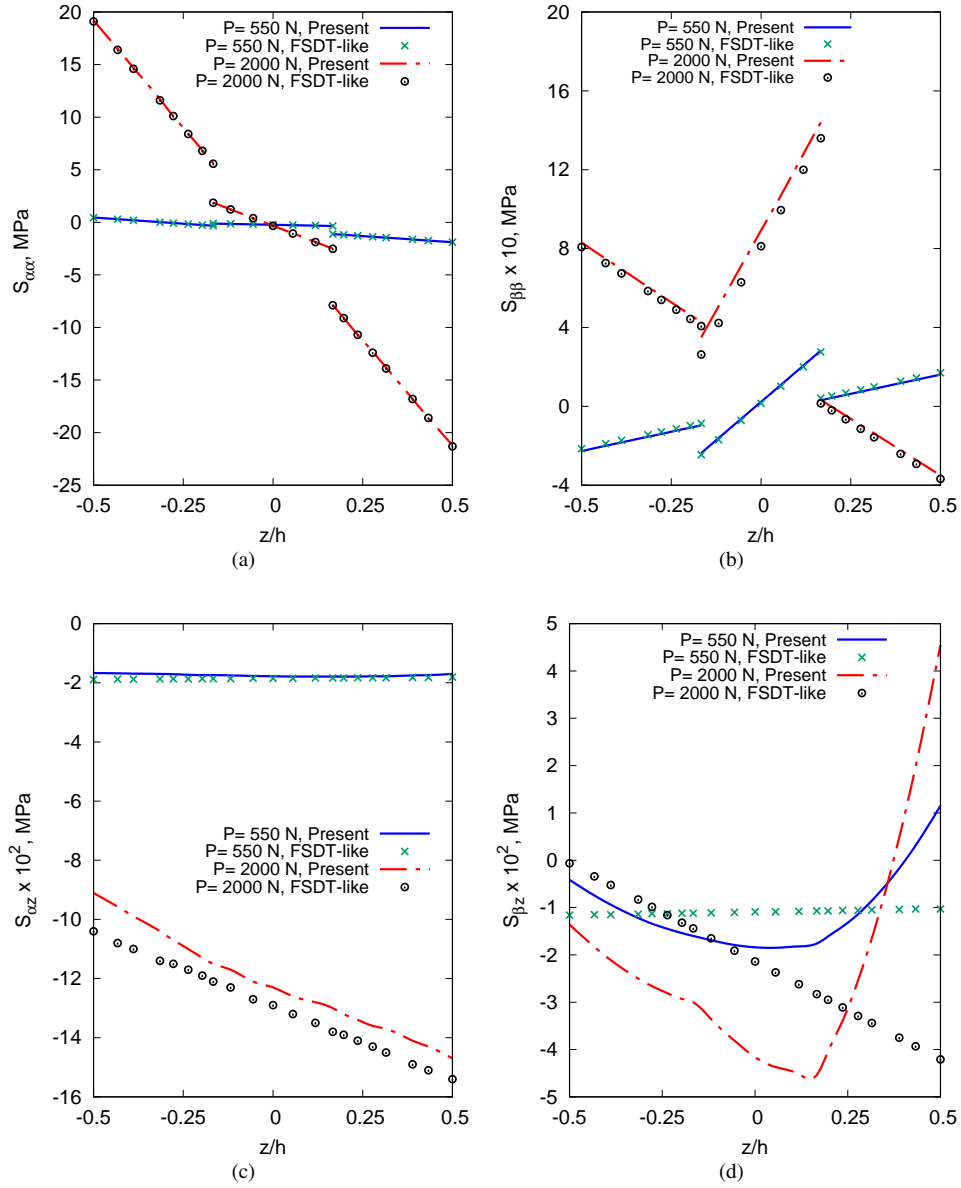


**Fig. 13** Through-the-thickness distribution of stresses for different loads at  $\alpha = 254.0$  mm and  $\beta = 127.0$  mm of the hinged cylindrical shell with  $10 \times 10Q9$  model. Lamination sequence  $[90^\circ, 0^\circ, 90^\circ]$ .

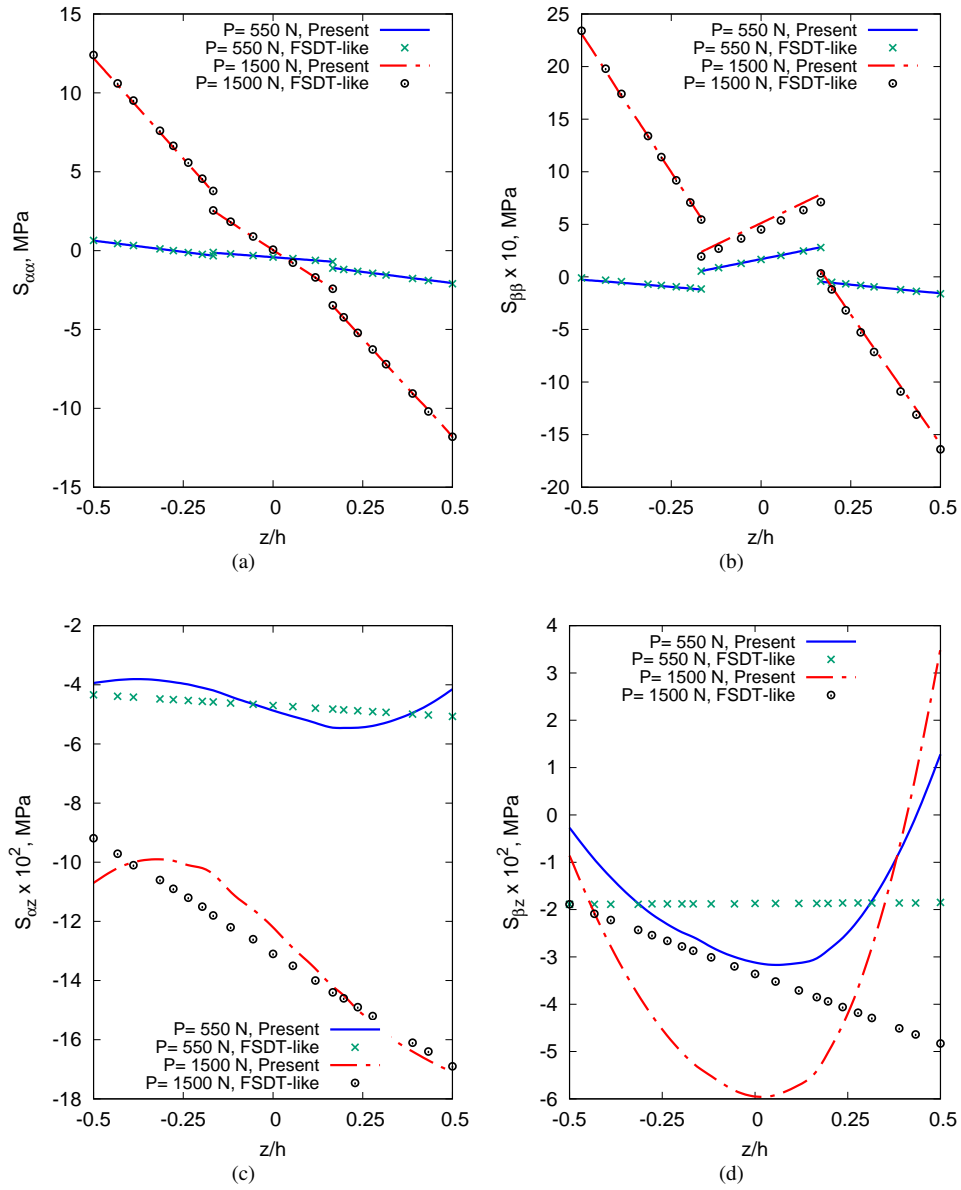


**Fig. 14** Through-the-thickness distribution of stresses for different loads at  $\alpha = 254.0$  mm and  $\beta = 127.0$  mm of the hinged cylindrical shell with  $10 \times 10Q9$  model. Lamination sequence:  $[45^\circ, 0^\circ, -45^\circ]$ .

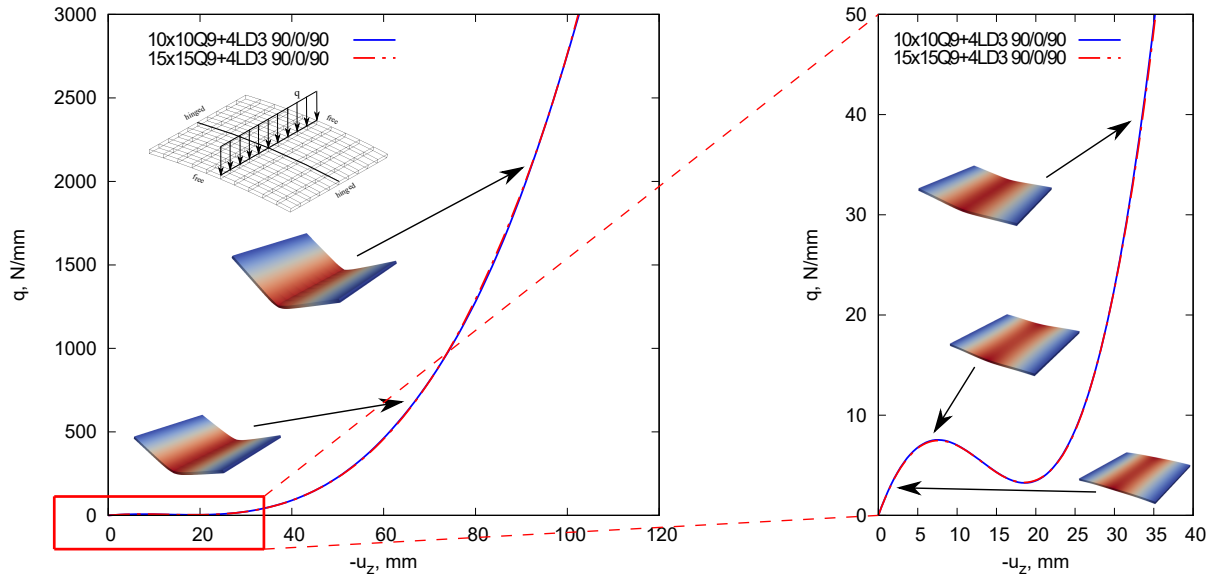


**Fig. 15** Equilibrium curve of the hinged cylindrical shell subjected to the line force. Lamination sequence:  $[90^\circ, 0^\circ, 90^\circ]$ .

## V. Conclusions

An advanced shell Finite Element (FE) for the geometrical nonlinear analysis of laminated structures has been discussed in this work. To account for classical to high-order kinematics, we have used the Carrera Unified Formulation (CUF) to express the FE arrays in a form that is independent of the structural theory order itself. No approximations have been made on the shell geometry and on the strain measure. In fact, the full Green-Lagrange strain tensor is used in a total Lagrangian description to obtain and discuss the through-the-thickness distribution of the Second Piola-Kirchhoff (PK2) stresses for different shell models, which represents the main objective of the work.

The results suggest that:

- The Equivalent Single Layer (ESL), as well as the Layerwise (LW) shell elements proposed, is able to accurately describe the nonlinear equilibrium curves of laminated composite structures in the case of moderate and large displacements. The results are in agreement with those from the literature;
- The proposed CUF-based LW models can predict interlaminar stress distributions in both linear and nonlinear equilibrium states with unprecedented accuracy. The results provided represent a benchmark for future studies;
- Classical theories, such as the first-order approximation, may bring to wrong and, eventually, unconservative stress distributions, especially in the nonlinear field. On the other hand, higher-order approximations, e.g., TE3 or TE4, may give good results in some circumstances.

Future works will investigate the extension to physical nonlinearities and advanced applications, such as structural failures involving postbuckling, shear crippling/kink band, and compression fracture.

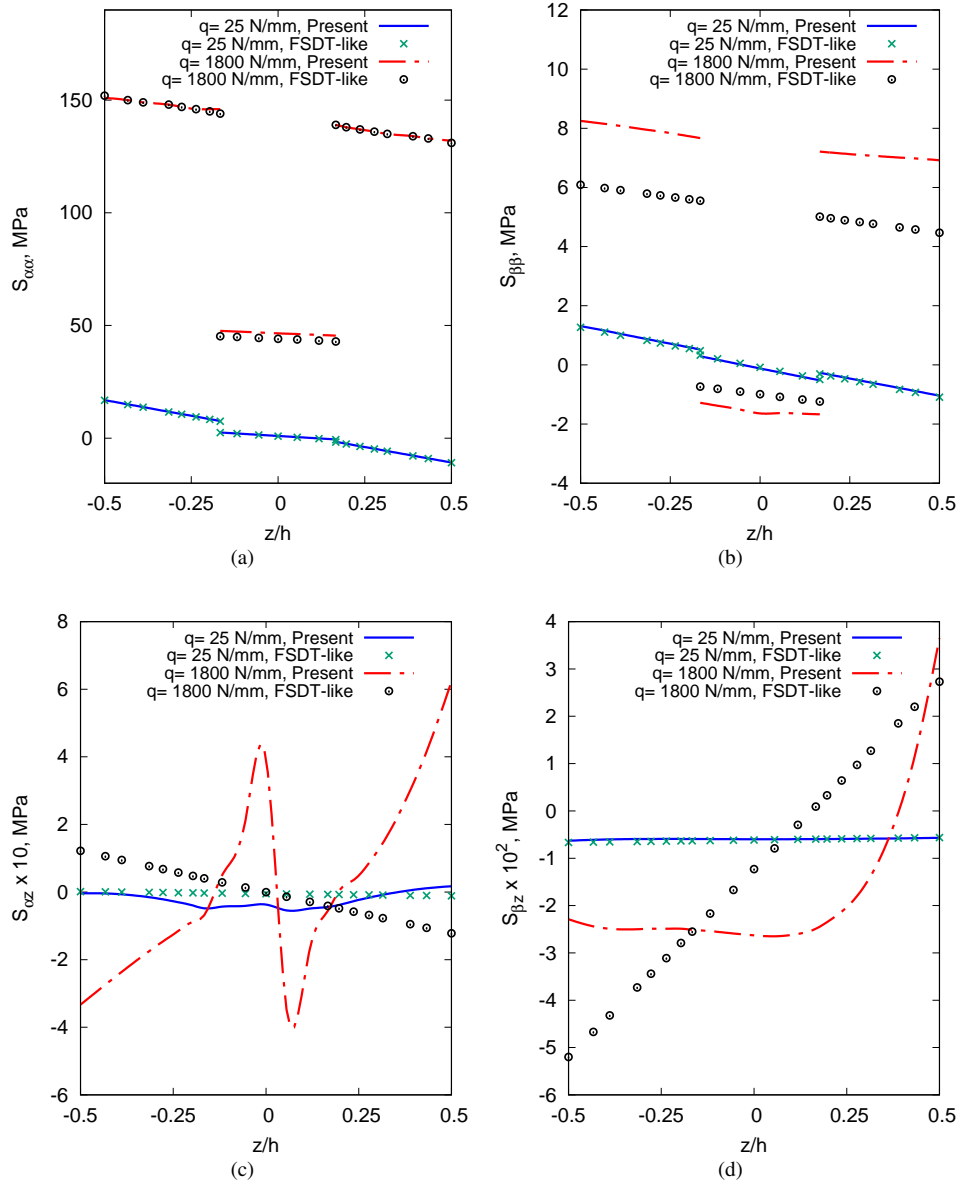


**Fig. 16** Through-the-thickness distribution of stresses for different loads at  $\alpha = 127.0$  mm and  $\beta = 245.0$  mm. Hinged cylindrical shell with  $10 \times 10 Q9$  model under a line load. Lamination sequence:  $[90^\circ, 0^\circ, 90^\circ]$ .

## References

- [1] Flügge, W., *Stresses in shells*, 2<sup>nd</sup> ed., Springer, Berlin, 1960.
- [2] Novozhilov, V., *Thin shell theory*, Noordhoff Ltd., Groningen, The Netherlands, 1964.
- [3] Calladine, C., *Theory of shell structures*, Cambridge University Press, 1989.
- [4] Niordson, F., *Shell theory*, Vol. 29, North-Holland Series in Applied Mathematics and Mechanics, 1985.
- [5] Basset, A., “On the extension and flexure of cylindrical and spherical thin elastic shells,” *Philosophical Transactions of the Royal Society of London.(A.)*, , No. 181, 1890, pp. 433–480.
- [6] Poisson, S., “Mémoire sur l’équilibre et le mouvement des corps élastiques,” *Mm. Acad. Sci. Instr. Fr.*, Vol. 8, 1829, pp. 357–570.
- [7] Love, A., “Mathematical Theory of Elasticity,” *Cambridge University Press*, 2013.
- [8] Mindlin, R., “Influence of rotary inertia and shear flexural motion of isotropic, elastic plates,” *Journal of Applied Mechanics*, Vol. 18, 1951, pp. 31–38.
- [9] Kirchhoff, G., “Über da gleichgewicht und die bewegung einer elastischen scheinbe,” *Journal Für Die Reine und Angewandte Mathematik*, Vol. 40, 1850, pp. 51–88.
- [10] Reissner, E., “The effect of transverse shear deformation on the bending of elastic plates,” *Journal of Applied Mechanics*, Vol. 12, 1945, pp. 69–76.
- [11] Cauchy, A., “Sur l’équilibre et le mouvement d’une plaque solide,” *Exerc. Math.*, Vol. 3, 1828, pp. 328–355.
- [12] Kapania, R., “A review on the analysis of laminated shells,” *ASME. Journal Pressure Vessel Technology*, Vol. 111, No. 2, 1989, pp. 88–96.
- [13] Reddy, J., and Liu, C., “A higher-order shear deformation theory of laminated elastic shells,” *International Journal of Engineering Science*, Vol. 23, No. 3, 1985, pp. 319–330.
- [14] Reddy, J., *Mechanics of Laminated Composite Plates and Shells: Theory and Analysis*, New York: CRC Press, 2004.
- [15] Başar, Y., Ding, Y., and Schultz, R., “Refined shear-deformation models for composite laminates with finite rotations,” *International Journal of Solids and Structures*, Vol. 30, No. 19, 1993, pp. 2611–2638. doi:[https://doi.org/10.1016/0020-7683\(93\)90102-D](https://doi.org/10.1016/0020-7683(93)90102-D).
- [16] Mashat, D., Carrera, E., Zenkour, A., Al Khateeb, S., and Lamberti, A., “Evaluation of refined theories for multilayered shells via Axiomatic/Asymptotic method,” *Journal of Mechanical Science and Technology*, Vol. 28, No. 11, 2014, pp. 4663–4672.
- [17] Jing, H., and Tzeng, K., “Refined shear deformation theory of laminated shells,” *AIAA Journal*, Vol. 31, No. 4, 1993, pp. 765–773. doi:<https://doi.org/10.2514/3.11615>.



- [18] Shu, X., “A refined theory of laminated shells with higher-order transverse shear deformation,” *International Journal of Solids and Structures*, Vol. 34, No. 6, 1997, pp. 673–683. doi:[https://doi.org/10.1016/S0020-7683\(96\)00048-0](https://doi.org/10.1016/S0020-7683(96)00048-0).
- [19] Carrera, E., “Theories and finite elements for multilayered, anisotropic, composite plates and shells,” *Archives of Computational Methods in Engineering*, Vol. 9, No. 2, 2002, pp. 87–140.
- [20] Cinefra, M., and Carrera, E., “Shell finite elements with different through-the-thickness kinematics for the linear analysis of cylindrical multilayered structures,” *International Journal for Numerical Methods in Engineering*, Vol. 93, No. 2, 2013, pp. 160–182. doi:<https://doi.org/10.1002/nme.4377>.
- [21] Petrolo, M., and Carrera, E., “Methods and guidelines for the choice of shell theories,” *Acta Mechanica*, 2020, pp. 1–40. doi:<https://doi.org/10.1007/s00707-019-02601-w>.
- [22] Cinefra, M., and Valvano, S., “A variable kinematic doubly-curved MITC9 shell element for the analysis of laminated composites,” *Mechanics of Advanced Materials and Structures, In Press*, Vol. 23, No. 11, 2016, pp. 1312–1325. doi:<https://doi.org/10.1080/15376494.2015.1070304>.
- [23] Li, G., Carrera, E., Cinefra, M., de Miguel, A., Pagani, A., and Zappino, E., “An adaptable refinement approach for shell finite element models based on node-dependent kinematics,” *Composite Structures*, Vol. 210, 2019, pp. 1–19. doi:<https://doi.org/10.1016/j.compstruct.2018.10.111>.
- [24] Reddy, J., “A review of refined theories of laminated composite plates,” *The Shock and Vibration Digest*, Vol. 22, No. 7, 1990, pp. 3–17.
- [25] Reddy, J., “On refined computational models of composite laminates,” *International Journal for Numerical Methods in Engineering*, Vol. 27, No. 2, 1989, pp. 361–382. doi:<https://doi.org/10.1002/nme.1620270210>.
- [26] Reddy, J., “A simple higher-order theory for laminated composite plates,” *Journal of Applied Mechanics*, Vol. 51, No. 4, 1984, pp. 745–752. doi:<https://doi.org/10.1115/1.3167719>.
- [27] Reddy, J., “A generalization of two-dimensional theories of laminated composite plates,” *Communications in Applied Numerical Methods*, Vol. 3, No. 3, 1987, pp. 173–180. doi:<https://doi.org/10.1002/cnm.1630030303>.
- [28] Owen, D., and Li, Z., “A refined analysis of laminated plates by finite element displacement methods — I. Fundamentals and static analysis,” *Computers & Structures*, Vol. 26, No. 6, 1987, pp. 907–914. doi:[https://doi.org/10.1016/0045-7949\(87\)90108-8](https://doi.org/10.1016/0045-7949(87)90108-8).
- [29] Reddy, J., “An evaluation of equivalent-single-layer and layerwise theories of composite laminates,” *Composite Structures*, Vol. 25, 1993, pp. 21–35. doi:[https://doi.org/10.1016/0263-8223\(93\)90147-I](https://doi.org/10.1016/0263-8223(93)90147-I).
- [30] Carrera, E., “Evaluation of layerwise mixed theories for laminated plates analysis,” *AIAA Journal*, Vol. 36, No. 5, 1998, pp. 830–839. doi:<https://doi.org/10.2514/2.444>.
- [31] Li, D., Qing, G., and Liu, Y., “A layerwise/solid-element method for the composite stiffened laminated cylindrical shell structures,” *Composite Structures*, Vol. 98, 2013, pp. 215–227. doi:<https://doi.org/10.1016/j.compstruct.2012.11.013>.

- [32] Guo, Y., Nagy, A., and Gürdal, Z., “A layerwise theory for laminated composites in the framework of isogeometric analysis,” *Composite Structures*, Vol. 107, 2014, pp. 447–457. doi:<https://doi.org/10.1016/j.compstruct.2013.08.016>.
- [33] Liew, K., Pan, Z., and Zhang, L., “An overview of layerwise theories for composite laminates and structures: Development, numerical implementation and application,” *Composite Structures*, 2019. doi:<https://doi.org/10.1016/j.compstruct.2019.02.074>.
- [34] Carrera, E., Pagani, A., and Valvano, S., “Shell elements with through-the-thickness variable kinematics for the analysis of laminated composite and sandwich structures,” *Composites Part B: Engineering*, Vol. 111, 2017, pp. 294–314. doi:<https://doi.org/10.1016/j.compositesb.2016.12.001>.
- [35] Zappino, E., Li, G., Pagani, A., and Carrera, E., “Global-local analysis of laminated plates by node-dependent kinematic finite elements with variable ESL/LW capabilities,” *Composite Structures*, Vol. 172, 2017, pp. 1–14. doi:<https://doi.org/10.1016/j.compstruct.2017.03.057>.
- [36] Varadan, T., and Bhaskar, K., “Review of different theories for the analysis of composites,” *Journal of Aerospace Society of India*, Vol. 49, 1997, pp. 202–208.
- [37] Reddy, J., and Robbins, D., “Theories and computational models for composite laminates,” *Applied Mechanics Review*, Vol. 47, 1994, pp. 147–165. doi:<https://doi.org/10.1115/1.3111076>.
- [38] Han, S., Tabiei, A., and Park, W., “Geometrically nonlinear analysis of laminated composite thin shells using a modified first-order shear deformable element-based Lagrangian shell element,” *Composite Structures*, Vol. 82, No. 3, 2008, pp. 465–474. doi:<https://doi.org/10.1016/j.compstruct.2007.01.027>.
- [39] Amabili, M., and Reddy, J., “A new non-linear higher-order shear deformation theory for large-amplitude vibrations of laminated doubly curved shells,” *International Journal of Non-Linear Mechanics*, Vol. 45, No. 4, 2010, pp. 409–418. doi:<https://doi.org/10.1016/j.ijnonlinmec.2009.12.013>.
- [40] Amabili, M., and Reddy, J., “The nonlinear, third-order thickness and shear deformation theory for statics and dynamics of laminated composite shells,” *Composite Structures*, Vol. 244, 2020, p. 112265. doi:<https://doi.org/10.1016/j.compstruct.2020.112265>.
- [41] Amabili, M., “Non-linearities in rotation and thickness deformation in a new third-order thickness deformation theory for static and dynamic analysis of isotropic and laminated doubly curved shells,” *International Journal of Non-linear Mechanics*, Vol. 69, 2015, pp. 109–128. doi:<https://doi.org/10.1016/j.ijnonlinmec.2014.11.026>.
- [42] Rivera, M., Reddy, J., and Amabili, M., “A new twelve-parameter spectral/hp shell finite element for large deformation analysis of composite shells,” *Composite Structures*, Vol. 151, 2016, pp. 183–196. doi:<https://doi.org/10.1016/j.compstruct.2016.02.068>.
- [43] Amabili, M., *Nonlinear Mechanics of Shells and Plates: Composite, Soft and Biological Materials*, Cambridge University Press, New York, USA, 2018.
- [44] Amabili, M., *Nonlinear Vibrations and Stability of Shells and Plates*, Cambridge University Press, New York, USA, 2008.

- [45] Boutagougua, D., and Djeghaba, K., "Evaluation of linear and geometrically nonlinear static and dynamic analysis of thin shells by flat shell finite elements," *Proceedings of World Academy of Science, Engineering and Technology*, World Academy of Science, Engineering and Technology (WASET), 2013, p. 359.
- [46] Chaudhuri, R., and Hsia, R., "Effect of thickness on large-deflection behavior of shells," *AIAA journal*, Vol. 37, No. 3, 1999, pp. 403–405. doi:<https://doi.org/10.2514/2.729>.
- [47] Chaudhuri, R., and Kim, D., "Effects of thickness and transverse shear modulus nonlinearity on the post-“yield” and post-localization response of an externally pressurized imperfect cross-ply ring," *Composite structures*, Vol. 88, No. 1, 2009, pp. 83–96. doi:[10.1016/j.compstruct.2008.02.016](https://doi.org/10.1016/j.compstruct.2008.02.016).
- [48] Kim, D., and Chaudhuri, R., "Effect of thickness on buckling of perfect cross-ply rings under external pressure," *Composite structures*, Vol. 81, No. 4, 2007, pp. 525–532. doi:<https://doi.org/10.1016/j.compstruct.2006.09.015>.
- [49] Kim, D., and Chaudhuri, R., "Postbuckling of moderately thick imperfect rings under external pressure," *Journal of Engineering Mechanics*, Vol. 132, No. 11, 2006, pp. 1273–1276. doi:[10.1061/\(ASCE\)0733-9399\(2006\)132:11\(1273\)](https://doi.org/10.1061/(ASCE)0733-9399(2006)132:11(1273)).
- [50] Klinkel, S., Gruttmann, F., and Wagner, W., "A continuum based three-dimensional shell element for laminated structures," *Computers & Structures*, Vol. 71, No. 1, 1999, pp. 43–62. doi:[https://doi.org/10.1016/S0045-7949\(98\)00222-3](https://doi.org/10.1016/S0045-7949(98)00222-3).
- [51] Dennis, S., and Palazotto, A., "Transverse shear deformation in orthotropic cylindrical pressure vessels using a higher-order shear theory," *AIAA Journal*, Vol. 27, No. 10, 1989, pp. 1441–1447. doi:<https://doi.org/10.2514/3.10283>.
- [52] Sze, K., Liu, X., and Lo, S., "Popular benchmark problems for geometric nonlinear analysis of shells," *Finite Elements in Analysis and Design*, Vol. 40, 2004, pp. 1551–1569. doi:<https://doi.org/10.1016/j.finel.2003.11.001>.
- [53] Librescu, L., "Refined geometrically nonlinear theories of anisotropic laminated shells," *Quarterly of Applied Mathematics*, Vol. 45, No. 1, 1987, pp. 1–22.
- [54] Carrera, E., "A class of two dimensional theories for multilayered plates analysis," *Atti Accademia delle Scienze di Torino, Memorie Scienze Fisiche*, Vol. 19-20, 1995, pp. 49–87.
- [55] Carrera, E., Giunta, G., Nali, P., and Petrolo, M., "Refined beam elements with arbitrary cross-section geometries," *Computers and Structures*, Vol. 88, No. 5–6, 2010, pp. 283–293. doi:<https://doi.org/10.1016/j.compstruc.2009.11.002>.
- [56] Pagani, A., and Carrera, E., "Unified formulation of geometrically nonlinear refined beam theories," *Mechanics of Advanced Materials and Structures*, Vol. 25, No. 1, 2018, pp. 15–31. doi:<https://doi.org/10.1080/15376494.2016.1232458>.
- [57] Wu, B., Pagani, A., Chen, W., and Carrera, E., "Geometrically nonlinear refined shell theories by Carrera Unified Formulation," *Mechanics of Advanced Materials and Structures*, 2019, pp. 1–21. doi:<https://doi.org/10.1080/15376494.2019.1702237>.
- [58] Green, A., and Zerna, W., *Theoretical elasticity*, Dover Publications, Inc. Mineola, New York, 1992.

- [59] Chaudhuri, R., “A New Three-Dimensional Shell Theory in General (Non-Lines of Curvature) Coordinates for Analysis of Curved Panels Weakened by Through/Part-Through Holes,” *Composite Structures*, Vol. 89, No. 1, 2009, pp. 321–332.
- [60] Bathe, K., and Bolourchi, S., “Large displacement analysis of three-dimensional beam structures,” *International Journal for Numerical Methods in Engineering*, Vol. 14, No. 7, 1979, pp. 961–986. doi:<https://doi.org/10.1002/nme.1620140703>.
- [61] Carrera, E., Pagani, A., Augello, R., and Wu, B., “Popular benchmarks of nonlinear shell analysis solved by 1D and 2D CUF-based finite elements,” *Mechanics of Advanced Materials and Structures*, 2020, pp. 1–12. doi:<https://doi.org/10.1080/15376494.2020.1728450>.
- [62] Bathe, K., *Finite element procedure*, Prentice Hall, Upper Saddle River, New Jersey, USA, 1996.
- [63] Hughes, T., *The finite element method: linear static and dynamic finite element analysis*, Dover Publications, Inc. Mineola, New York, 2012.
- [64] Carrera, E., Cinefra, M., Petrolo, M., and Zappino, E., *Finite Element Analysis of Structures through Unified Formulation*, John Wiley & Sons, New York, USA, 2014.
- [65] Carrera, E., Giunta, G., and Petrolo, M., *Beam Structures: Classical and Advanced Theories*, John Wiley & Sons, 2011. doi:[10.1002/9781119978565](https://doi.org/10.1002/9781119978565).
- [66] Reddy, J., *An Introduction to Nonlinear Finite Element Analysis: with applications to heat transfer, fluid mechanics, and solid mechanics*, Oxford University Press, Oxford, 2014.
- [67] Carrera, E., “A study on arc-length-type methods and their operation failures illustrated by a simple model,” *Computers & Structures*, Vol. 50, No. 2, 1994, pp. 217–229. doi:[https://doi.org/10.1016/0045-7949\(94\)90297-6](https://doi.org/10.1016/0045-7949(94)90297-6).
- [68] Crisfield, M., “A fast incremental/iterative solution procedure that handles “snap-through”,” *Computers & Structures*, Vol. 13, No. 1, 1981, pp. 55–62. doi:<https://doi.org/10.1016/B978-0-08-027299-3.50009-1>.
- [69] Carrera, E., Cinefra, M., Petrolo, M., and Zappino, E., *Finite Element Analysis of Structures through Unified Formulation*, John Wiley & Sons, Chichester, West Sussex, UK, 2014.